



# Measuring Substrate-Independent Young's Modulus of Low- $\kappa$ Films by Instrumented Indentation

## Application Note

Jennifer Hay

### Introduction

In digital circuits, insulating dielectrics separate the conducting parts (wire interconnects and transistors) from one another. As components have scaled and transistors have gotten closer and closer together, the insulating dielectrics have thinned to the point where charge build-up and crosstalk adversely affect the performance of the device. It is this reduction in scale which drives the need for insulating materials with lower dielectric constant. A 'low- $\kappa$ ' material is one with a small value for dielectric constant relative to silicon dioxide ( $\text{SiO}_2$ )—a former dielectric of choice. The dielectric constant of  $\text{SiO}_2$  is 3.9. This number is the ratio of the permittivity of  $\text{SiO}_2$  divided by permittivity of vacuum,  $\epsilon_{\text{SiO}_2}/\epsilon_0$ , where  $\epsilon_0 = 8.854 \times 10^{-6} \text{ pF}/\mu\text{m}$ . There are many materials with lower dielectric constants, but few of them can be suitably integrated into a semiconductor manufacturing process [1].

At the extreme, dry air (20°C, 1 atm) has a dielectric constant of 1.00059 [2], but dry air cannot keep conducting materials mechanically separated, so it cannot be used as an insulator. But as one incorporates material for structure, the dielectric constant also increases. So the optimization problem in materials development for semiconductors is to lower the permittivity of the dielectric material as far as possible without compromising mechanical integrity, as quantified by the Young's modulus. Generally, processes purposed for reducing permittivity (such as pore introduction) also have the effect of reducing Young's modulus.

Instrumented indentation is commonly employed in the semiconductor industry to measure the Young's modulus of low- $\kappa$  films deposited on silicon wafers. Two typical wafers are shown in Figure 1. Commonly, these films are less than 200 nm thick. Without any correction for influence of the underlying silicon substrate, one faces a compromise between uncertainty and error. At very small displacements, the error due to the substrate influence is small, but the uncertainty is greater due to surface roughness, tip variations, vibration, temperature variations, etc. As indentation depth increases, the uncertainty decreases, but the error due to substrate influence increases. The issue is even more complex because many low- $\kappa$  films present a "skin" with properties that are not representative of the bulk of the film. When testing

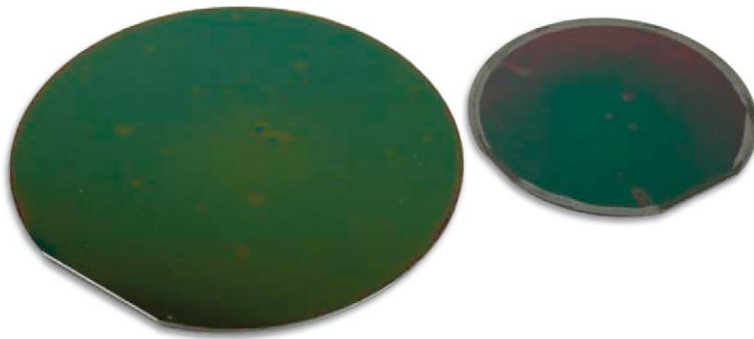


Figure 1. Whole silicon wafers, coated with low- $\kappa$  materials.

such a film by instrumented indentation, the near-surface data are affected by this skin, and data at larger depths are affected by the substrate, leaving no domain in which the properties of the film alone can be obtained. Thus, the purpose of this work was to apply an analytic model to the analysis of low- $\kappa$  films tested by instrumented indentation in order to obtain the Young's modulus of the film alone. In a previous application note, such a model was introduced and verified by finite-element analysis [3]. Hereafter, this model will be called the "Hay-Crawford" model.

### Theory

The Hay-Crawford model provides an analytic means for accounting for substrate influence on measured modulus. The model presumes that apparent modulus has already been determined. Here, "apparent modulus" means modulus calculated according to the method of Oliver and Pharr [4]. This method has been explained in detail elsewhere [5, 6].

The Hay-Crawford model is expressed in terms of shear modulus; the general relation between Young's modulus ( $E$ ), shear modulus ( $\mu$ ), and Poisson's ratio ( $\nu$ ) is  $E = 2\mu(1+\nu)$ . The Hay-Crawford model presumes that the film acts in series and in parallel with the substrate as illustrated in Figure 2. Thus, the apparent (substrate-affected) shear modulus ( $\mu_a$ ) is related to the shear modulus of the film ( $\mu_f$ ) and that of the substrate ( $\mu_s$ ) through this expression:

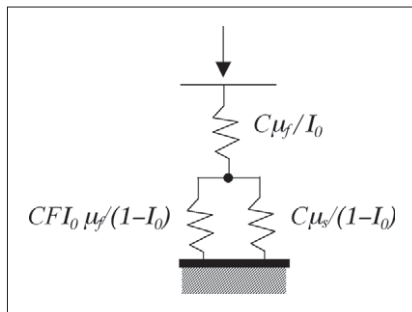
$$\frac{1}{\mu_a} = (1-I_0) \frac{1}{\mu_s + 0.0626I_0\mu_f} + I_0 \frac{1}{\mu_f}. \quad (\text{Eq. 1})$$


Figure 2. Schematic of the proposed model. Top spring represents the action of the film. Bottom two springs represent the film and substrate acting in parallel.

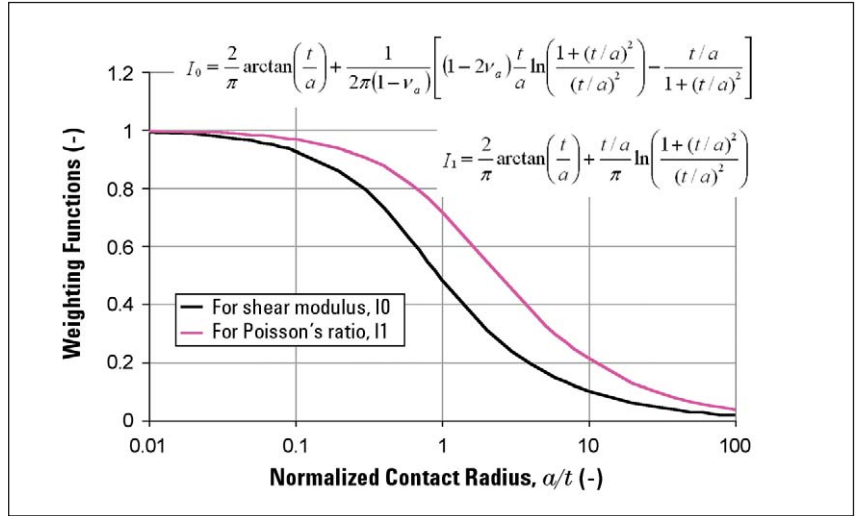


Figure 3. Weighting functions for shear modulus ( $I_0$ ) and Poisson's ratio ( $I_1$ ).

The weighting function,  $I_0$ , is due to Gao [7]; it provides for a smooth transition between the influence of the film and that of the substrate. The expression for  $I_0$  is provided in Figure 3 where it is plotted against normalized contact radius ( $a/t$ ).

Thus, the shear modulus of the film is calculated from the apparent value by solving Eq. 1 for  $\mu_f$ :

$$\mu_f = \frac{-B + \sqrt{B^2 - 4AC}}{2A}, \quad \text{where} \quad (\text{Eq. 2})$$

$$\begin{aligned} A &= 0.0626I_0/\mu_a \\ B &= \mu_s/\mu_a + I_0 - 1 - 0.0626I_0^2 \\ C &= -I_0/\mu_s \end{aligned}$$

Finally, the Young's modulus of the film is calculated from the shear modulus and Poisson's ratio as

$$E_f = 2\mu_f(1+\nu_f). \quad (\text{Eq. 3})$$

Calculation of  $\mu_a$  from standard indentation results for use in Eq. 1 requires a value for Poisson's ratio. The weighting function  $I_0$  also utilizes Poisson's ratio. But what value should be used—that of the film or that of the substrate? To be sure, this problem is of second order, but Gao also suggest a weighting function,  $I_1$ , for handling the transition in Poisson's ratio, so that the apparent Poisson's ratio,  $\nu_a$ , is calculated as

$$\nu_a = 1 - \frac{(1-\nu_s)(1-\nu_f)}{1 - (1-I_1)\nu_f - I_1\nu_s}. \quad (\text{Eq. 4})$$

Eq. 4 provides the value for Poisson's ratio used in the calculation of  $\mu_a$  and  $I_0$ . It should be noted that if film and substrate have the same Poisson's ratio (that is, if  $\nu_s = \nu_f = \nu$ ), then Eq. 4 reduces to  $\nu_a = \nu$ . The expression for  $I_1$  is also provided in Figure 3 where it is plotted against normalized contact radius.

### Experimental Method Samples

Two low- $\kappa$  films on silicon were tested; the thickness of the first film was 1007nm and the thickness of the second film was 445nm. Figure 4 shows the two samples mounted for testing. In a previous application note, results were reported for these same samples, but without any accounting for substrate influence [8]. In this work, we compare results obtained by the Hay-Crawford model to those previously reported.

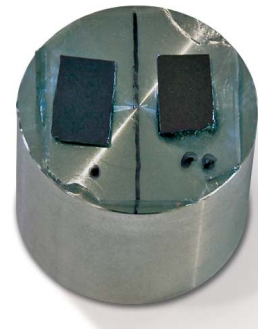


Figure 4. Two low- $\kappa$  samples, as mounted for testing in the G200.

### Equipment and Procedure

The two low- $\kappa$  samples were tested in an Agilent lab with an Agilent G200 NanoIndenter, utilizing the CSM option and a DCM II head fitted with a Berkovich indenter. Results were achieved using the NanoSuite test method “G-Series DCM CSM for Thin Films”. This test method implements the Hay-Crawford model to achieve substrate-independent measurements of Young’s modulus. It should be noted that this method does not correct measurements of *hardness* for substrate influence. However, hardness measurements are generally less sensitive to substrate influence, because the extent of the plastic field is much smaller than the extent of the elastic field. Even when there is a substantial difference between film hardness and substrate hardness, the hardness measured at 10% of the film thickness usually manifests negligible substrate influence.

Agilent NanoIndenter have been the industry choice for thin-film testing precisely because of the *continuous stiffness measurement* (CSM) option, which measures elastic contact stiffness ( $S$ ) dynamically. With the CSM option, every indentation test returns complete depth profiles of Young’s modulus and hardness. Using this option, eight tests were performed on each low- $\kappa$  sample. Loading was controlled such that the loading rate divided by the load ( $P'/P$ ) remained constant at 0.05/sec; loading was terminated at a penetration depth of 200 nm or greater. The excitation frequency was 75 Hz, and the excitation amplitude was controlled such that the displacement amplitude remained constant at 1 nm.

### Results and Discussion

Results are summarized in Table 1. Figure 5 and Figure 6 show the Young’s modulus as a function of penetration depth for each sample. The blue traces are the uncorrected values; these show what would be achieved without any correction for substrate influence using a standard NanoSuite test method such as “G-Series DCM CSM Standard Hardness, Modulus, and Tip Cal”. These blue traces show

1	2	3	4	5	6	7	8	9
			Results, Standard			Results, by Eqs. 1-3		
Sample	N	Thickness nm	Range* nm	$E_a$ GPa	$\sigma(E_a)$ GPa	Range** nm	$E_f$ GPa	$\sigma(E_f)$ GPa
low- $\kappa$ 1	8	1007	35-40	4.69	0.07	95.9-105.4	4.34	0.06
low- $\kappa$ 2	8	445	25-30	8.23	0.13	42.2-46.8	7.46	0.12

Table 1. Summary of results.

\* Selected by eye

\*\* Corresponds to 9.5%-10.5% of film thickness

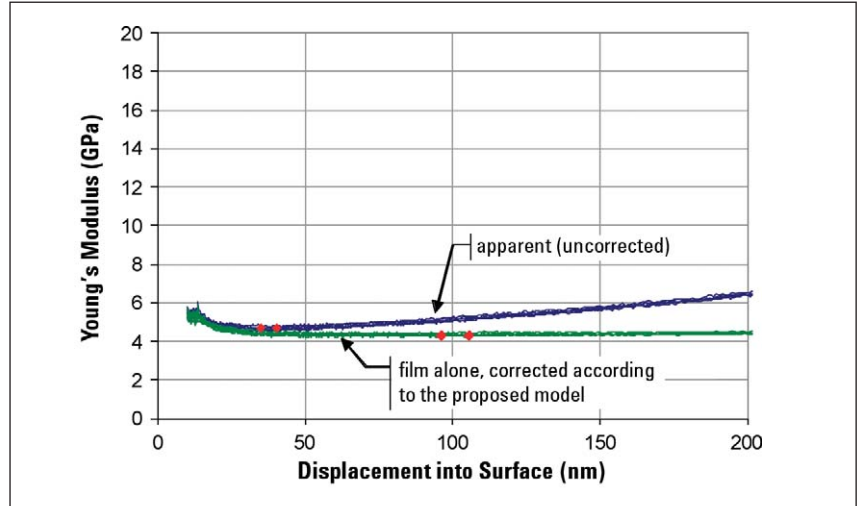


Figure 5. Low- $\kappa$  1 on silicon substrate,  $t_f = 1007$  nm.

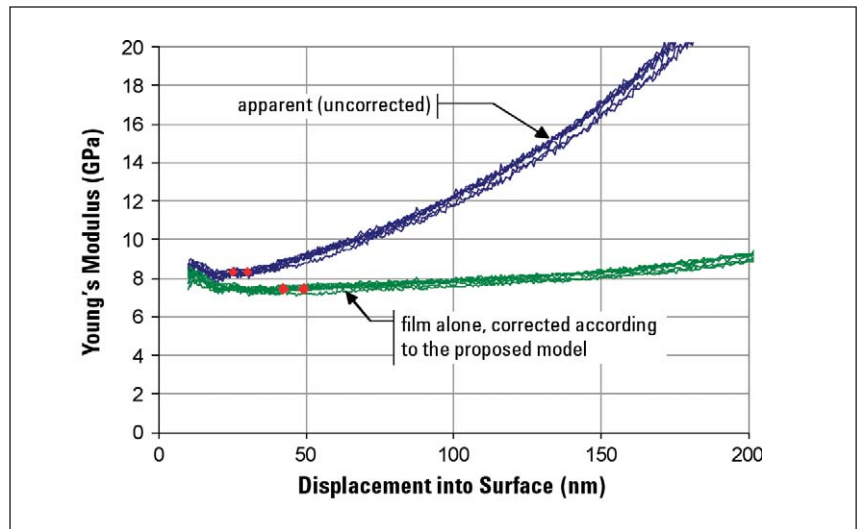


Figure 6. Low- $\kappa$  2 on silicon substrate,  $t_f = 445$  nm.

Young’s modulus increasing as a function of displacement, because the silicon substrate, which is much stiffer, increasingly affects the measurement. The effect is more pronounced for thinner film; the blue traces increase most rapidly for the “low- $\kappa$  2” sample, because it is the thinnest film tested in this work. The red diamonds show

the range used to calculate the (uncorrected) Young’s moduli in the fifth column of Table 1. Logistically, these diamonds are placed by the user so as to select data which are, in the user’s judgment, free from both surface anomalies and substrate influence.

The green traces of Figure 5 and Figure 6 are the values calculated according to Eqs. 1-3. The red diamonds show the range used to calculate the Young's moduli in the eighth column of Table 1, but diamonds were placed automatically by the software at 9.5% and 10.5% of the film thickness, respectively, so as to reduce the amount of user judgment involved in deriving results. The corrected Young's moduli cited at 10% of the film thickness (Table 1, column 8) are significantly lower than what was previously reported for these samples (Table 1, column 5).

Another important observation is that when a correction for substrate influence is employed, the results can be taken from deeper into the film where surface anomalies have less influence. As a result, the standard deviations are smaller, as can be seen by comparing values in the sixth and ninth columns of Table 1.

## Conclusions

The Agilent G200 NanoIndenter with a DCM II head is the industry choice for these measurements because of its high-precision, speed, ease of use, and the CSM option, which delivers properties as a continuous function of penetration depth. In this work, NanoSuite Explorer was used to implement an analytic model which accounts for substrate influence. Test methods with this analysis are now available to customers with NanoSuite Professional.

Having a model which corrects for substrate influence affords several practical advantages:

- Reported moduli are for the film alone,
- Less user influence, because depth range for calculating moduli does not have to be selected "by eye", and
- Smaller uncertainty in results, because moduli are taken from deeper into the film.

## References

1. [http://en.wikipedia.org/wiki/Low-K#Spin-on\\_organic\\_polymeric\\_dielectrics](http://en.wikipedia.org/wiki/Low-K#Spin-on_organic_polymeric_dielectrics)
2. <http://hyperphysics.phy-astr.gsu.edu/Hbase/tables/diel.html>
3. J.L. Hay, "A new model for measuring substrate-independent Young's modulus of thin films by instrumented indentation," Agilent Technologies application note (2010).
4. W.C. Oliver and G.M. Pharr, "An improved technique for determining hardness and elastic modulus using load and displacement sensing indentation experiments," *J. Mater. Res.*, **7**(6): 1564–1583 (1992).
5. J.L. Hay, "Introduction to instrumented indentation testing," *Experimental Techniques* **33**(6): 66-72 (2009).
6. J.L. Hay, P. Agee, and E.G. Herbert, "Continuous stiffness measurement during instrumented indentation testing," *Experimental Techniques* **34**(3):86-94 (2010).
7. H. Gao, C.-H. Chiu, and J. Lee, "Elastic contact versus indentation modeling of multi-layered materials. *Int. J. Solids Structures*," **29**:2471-2492 (1992).
8. J.L. Hay, "Young's modulus of dielectric 'low- $\kappa$ ' materials," Agilent Technologies application note (2010).

## Nano Mechanical Systems from Agilent Technologies

Agilent Technologies, the premier measurement company, offers high-precision, modular nano-measurement solutions for research, industry, and education. Exceptional worldwide support is provided by experienced application scientists and technical service personnel. Agilent's leading-edge R&D laboratories ensure the continued, timely introduction and optimization of innovative, easy-to-use nanomechanical system technologies.

[www.agilent.com/find/nanoindenter](http://www.agilent.com/find/nanoindenter)

### Americas

Canada	(877) 894 4414
Latin America	305 269 7500
United States	(800) 829 4444

### Asia Pacific

Australia	1 800 629 485
China	800 810 0189
Hong Kong	800 938 693
India	1 800 112 929
Japan	0120 (421) 345
Korea	080 769 0800
Malaysia	1 800 888 848
Singapore	1 800 375 8100
Taiwan	0800 047 866
Thailand	1 800 226 008

### Europe & Middle East

Austria	43 (0) 1 360 277 1571
Belgium	32 (0) 2 404 93 40
Denmark	45 70 13 15 15
Finland	358 (0) 10 855 2100
France	0825 010 700*
	*0.125 €/minute
Germany	49 (0) 7031 464 6333
Ireland	1890 924 204
Israel	972-3-9288-504/544
Italy	39 02 92 60 8484
Netherlands	31 (0) 20 547 2111
Spain	34 (91) 631 3300
Sweden	0200-88 22 55
Switzerland	0800 80 53 53
United Kingdom	44 (0) 118 9276201

Other European Countries:

[www.agilent.com/find/contactus](http://www.agilent.com/find/contactus)

Product specifications and descriptions in this document subject to change without notice.

© Agilent Technologies, Inc. 2011  
Printed in USA, October 5, 2011  
5990-6508EN